Ultrasonic 3D Position Estimation using a Single Base Station

Esko Dijk[1,2], Kees van Berkel[1,2], Ronald Aarts[2], and Evert van Loenen[2]

[1] Eindhoven University of Technology,
Postbus 513, 5600 MB Eindhoven, The Netherlands
esko@ieee.org
[2] Philips Research Laboratories Eindhoven,
Prof. Holstlaan 4, 5656 AA Eindhoven, The Netherlands
evert.van.loenen@philips.com

Abstract. In indoor context awareness applications the location of people, devices or objects is often required. Ultrasound technology enables high resolution indoor position measurements. A disadvantage of state-of-the-art ultrasonic systems is that several base stations are required to estimate 3D position. Since fewer base stations leads to lower cost and easier setup, a novel method is presented that requires just one base station. The method uses information from acoustic reflections in a room, and estimates 3D positions using an acoustic room-model. The method has been implemented, and verified within an empty room. It can be concluded that ultrasonic reflection data provides useful clues about the 3D position of a device.

1 Introduction

In many context aware computing applications, the locations of people, devices or objects is part of the required context information. For some applications, also the orientation of devices [1], people or objects plays a role. Typically, indoor applications require higher resolution than 'on the move' and outdoor applications, anywhere between room-size and sub-centimeter. Within the PHENOM project [2] we focus on the *in-home* application area. Context awareness in the home can make technology more enjoyable and easy-to-use or enable new experiences that users may find attractive. Several application scenarios were developed in our project that require location information. For example, one scenario enables users to intuitively 'move' content from any handheld or fixed display device, to any other nearby display. Proximity between displays can be determined by using the devices' mutual positions and orientations. A second application is the control of light, music and atmosphere settings in the living room, based on the positions of small devices or 'smart objects' that users can move around. For these applications, we need a resolution of at least one meter.

The required resolution is much higher than wide-area systems –like GPS– can deliver indoors at the moment. Therefore many research and commercial

systems exist that can provide indoor location information at a finer scale. Systems based on either radio (RF) or ultrasonic technologies are most popular and promising at the moment. RF systems typically cover wider areas like buildings, but have difficulties reaching high accuracy [3, 4]. Ultrasonic systems can routinely offer very high (centimeter) resolution as shown in the Bat [5], Cricket [1], Dolphin [6], and InterSense [7] systems. But they have a limited operating range which makes deployment throughout a building difficult. Because of the potential high resolution, we are investigating ultrasound technology for home applications.

State-of-the-art ultrasonic systems are based on calculating distances (or distance-differences) by measuring ultrasound time-of-flight. A position estimate can be obtained using triangulation algorithms with these distances as inputs. A disadvantage of this approach is that several units of infrastructure are required, to generate sufficient input for a triangulation algorithm. Generally, four base stations (BS) are needed in a non-collinear setup to estimate 3D position. For special cases we can do with three, for example three ceiling-mounted BSs. However, more than three or four BSs are often employed for increased robustness [5, 1], or the ability to estimate speed-of-sound from measurements [1]. For RF systems the same problem exists. The need for high resolution leads to large numbers of units within an infrastructure (e.g. [3]), increasing installation and maintenance (e.g. battery replacement) effort and cost.

An important goal of indoor positioning systems research is to realise ubiquitous deployment in an economically viable way. This means that a technology is preferably cheap, easy to set up, and low-maintenance. We argue that these requirements can be better met if the infrastructure is minimal. Fewer BSs could mean lower cost and easier setup. The resulting research question is whether a 3D positioning system can work with fewer BSs, and if in the extreme case a single BS (of small size) would be sufficient. Two concepts emerged to realise such a single-base-station positioning system. The first concept makes use of always-present ultrasonic reflections against the walls and ceiling of a room. Considering ultrasonic emissions coming from a source somewhere in the room, reflections can be considered as coming from *virtual sources* at other positions. The virtual sources might replace real sources, thereby reducing the number of BSs. The second idea was to employ acoustic array techniques [8] that are well-known in source localisation research.

The first concept is the topic of this paper. A new method was developed that uses reflections for 3D positioning, requiring a single base station per room. An introduction to the *signature matching* method is given in section 2. An acoustic model that plays a central role in the method, will be developed in section 3. The method will be presented in more detail in section 4. An implementation of the method and experimental work are described in section 5 and conclusions are given in section 6.

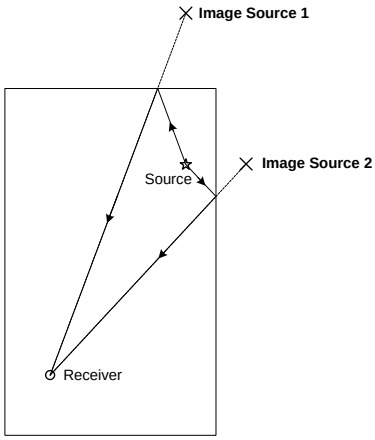

Fig. 1. 2D top view of a room, containing one acoustic source and one receiver. Two acoustic reflections (arrows) and associated image sources (crosses) are shown.

2 Method overview

The new method is based on the idea of using ultrasonic reflections off surfaces (walls, floor and ceiling) within a room. To clarify this, Fig. 1 shows a top view of a room, with one acoustic source and one receiver. The source emits a direct sound field to the receiver, but sound also reflects off the four walls and arrives at the receiver indirectly. Two such indirect (reflected) acoustic rays are shown in the figure. From ray acoustics theory (to be introduced in section 3.3) it is known that reflections can be modelled as emissions from so-called *image sources* located outside the physical room boundaries. Their positions can be constructed by a mirror-symmetry operation with respect to the room boundary. Two image sources, associated to the example reflected rays, are shown in the figure. Many more image sources exist, like ceiling and floor reflections and higher-order reflections (e.g. wall–ceiling–wall). The combined effect of reflections can be observed in Fig. 2, which shows a processed acoustic measurement. The many peaks in this graph are caused by reflections, arriving at the receiver at different moments in time. Such a pattern of reflections was observed to be dependent on the 3D receiver position and orientation. These patterns were named *signatures* because of the information they contain about receiver position and orientation. The signature shown was obtained using the procedure described in section 5.1.

Let's assume for now that the acoustic source is a base station (BS) fixed at a known position and the receiver is a mobile device, with an unknown position to be measured. It is expected that the image sources can be used as if they are 'virtual base stations' (VBS). The combined information from BS and VBSs might enable calculation of 3D receiver position. The problem with VBSs is that we can neither identify nor distinguish them. For example, for the peaks in Fig.

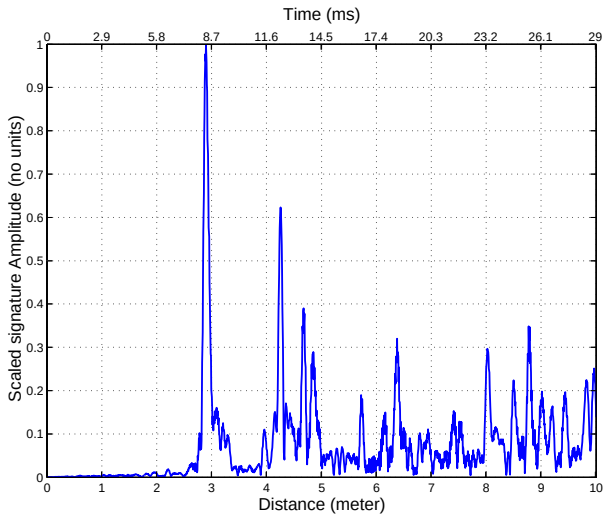

Fig. 2. Measured signature at position $x_R = (2.60, 1.70, 1.27)$. The horizontal axes show time (top) and the corresponding distance interval of $[0, 10]$ m. Signatures are obtained by the procedure in section 5.1.

2 it is not known by which VBS they were 'transmitted'. As a result, standard triangulation algorithms can not be applied. Estimating the identity of peaks would be required first, but this is a very difficult problem.

Concluding, we have not found any method yet that can directly calculate a 3D position from a given signature. However, the reverse is easier: computing a signature, given a 3D position. This fact is exploited by the *signature matching* method. It simply tries many mobile device 3D candidate positions and predicts their signatures. Then, all predicted signatures are compared or *matched* to the measured signature and the best match is selected. The details of the method will be discussed in section 4.

3 Acoustical system model

Acoustical models of both the positioning system and the room are needed, to be able to predict an acoustic signal at a certain position in a room. Such predicted signals are needed to compare to measured signals, as explained in the previous section. The acoustical model includes a transmitter, a receiver and the room. In section 3.1 the transducers are modelled, in section 3.2 acoustical phenomena indoors are listed, and in section 3.3 we show how a box-shaped room can be modelled. Finally section 3.4 combines these elements into a system model.

3.1 Transducers model

For the implementation, piezo-electric ultrasound transducers were selected. They are cheap, have a small form factor, and operate on low voltage and low power. Each type of transducer has specific frequency-dependent behaviour. Piezo transducers can be conveniently modelled as linear systems [9], e.g. represented by an impulse response. The transmitter/receiver impulse responses are part of the system model. They can be obtained by measurement, or by modelling [9].

Most ultrasonic transmitters are directional, designed to emit acoustic energy mainly within a narrow beam from the front. Likewise, receivers are most sensitive at the front. This directionality can be captured in the *normalised beampattern function* $D_N(\theta)$ of the transducer, where θ is the angle with respect to the transducer axis. Maximum amplitude occurs on-axis, when $D_N(0) = 1$. The beampattern for disc-shaped piezo transducers can be approximated by that of an ideal circular piston [8]. However, the piston model had to be extended to account for the protective metal casing that surrounds the piezo element. We used an empirical damping factor K_d that was found to correspond well to measured amplitudes:

$$K_d(\theta) = 0.525 + 0.475 \ \cos(\theta) \ . \tag{1}$$

3.2 Acoustical phenomena indoors

In this section, the ultrasound phenomena that are part of the acoustic room model are briefly presented.

Ultrasound propagation in air. Distance can be calculated using time-of-flight measurement and the speed of sound c in air. However, c varies with air temperature [10]. Distance errors can be caused due to imperfect knowledge of the current room temperature. We will assume that room temperature is either approximately known or measured.

Acoustic waves are attenuated over distance due to *geometric spreading loss* and *atmospheric absorption loss*. The spreading loss is the well-known acoustic pressure loss of r^{-1} over distance r [9]. The absorption loss is caused by lossy molecular interaction processes [9]. It can be high for ultrasound in air, and limits the usable range of ultrasonic distance measurement. The loss can be calculated using the *absorption loss factor* α in dB/meter. α depends on temperature, relative humidity, and the frequency of sound in a non-linear manner. Equations to calculate α [11] are part of the model. The relative humidity parameter can be measured or simply set to a default value. Automatic calibration of α is possible from base station measurements, but outside the scope of this paper.

Reflection and diffraction. A sound wave in air incident to a boundary surface, such as a wall or ceiling, will cause a reflected wave and a transmitted wave. The latter is usually absorbed within the medium. For ideal homogeneous

materials with smooth surfaces, theory predicts *specular reflection* [10]: angle of incidence equals angle of reflection. The reflected wave continues in air, with lower amplitude than the incoming wave due to absorption. The *reflection factor* Γ, reflected wave amplitude divided by incoming wave amplitude, models this. Value for Γ are difficult to calculate precisely, since typical room boundary materials are not smooth and homogeneous. From measurements we observed that for typical building materials there is little reflection loss ($\Gamma \approx 1$) at ultrasonic frequencies around 40 kHz. However, for soft materials such as curtains or carpet (e.g. $\Gamma \approx 0.3$), the loss can be substantial. An estimation $\Gamma = 1$ was used in our model.

Another effect is *diffraction*, the deflecting or 'bending' of acoustic waves around obstacles. In a typical room, diffraction is mostly unpredictable, because we do not know the sizes and positions of the obstacles (like furniture and people). Therefore we can not model diffraction.

3.3 Room impulse response model

Rooms exist in many shapes, but home and office rooms are often approximately box shaped. Another common shape is the L-shaped room, which is acoustically more complicated. We focus on box-shaped rooms, which have six boundary surfaces (four walls, ceiling and floor). The goal of the model presented here is to predict the impulse response of a room $h(t, \mathbf{p})$ as a function of relevant parameters, described by a parameter vector $\mathbf{p}$. It includes the room size and shape (assumed to be known), transmitter and receiver positions and orientations, surface reflection factors, and room temperature and humidity. In practice the room response is a complicated function of other parameters as well, such as people/objects/furniture in the room and room materials. However, a 'minimal' room model of an empty room can be constructed that only includes the six boundary surfaces. This is a standard approach in room acoustics. To model a room the *image method* was applied, because for box-shaped rooms an impulse response for short durations can be calculated efficiently using the model of Allen and Berkley [12]. See section 2 for an explanation of the image sources concept or [12, 10] for details.

The image method is based on the *ray acoustics* [10] approximation of acoustic waves. For ray acoustics models of arbitrarily shaped rooms, the room impulse response h in a time interval $[0, t_e]$ can be written as a sum of N independent rays arriving at the receiver:

$$h(t, \mathbf{p}) = \sum_{i=1}^{N} a_i \cdot \delta(t - d_i/c) \tag{2}$$

where ray d_1 is the line-of-sight and (N-1) rays are reflections, d_i is the distance the i-th ray travels, a_i is the amplitude of the i-th ray arriving at the receiver, c is the speed of sound and δ the Dirac delta function. This equation holds for arbitrary transmitted signal shapes. d_i, a_i and c depend on the parameter vector $\mathbf{p}$. For a box-shaped room the details for calculating distances d_i using

the image method are given in [12]. The amplitudes a_i can be described in terms of acoustic pressure, taking into account the pressure loss over distance (section 3.2), pressure loss due to reflections (section 3.2) and the attenuation caused by the orientations of both transducers (section 3.1).

3.4 System impulse response model

In sections 3.1 to 3.3 it was shown that impulse responses of transmitter, receiver and the room can be obtained. To obtain a system impulse response we simply concatenate these three by convolution:

$$h(t, \mathbf{p}) = h_T(t) * h_{Rm}(t, \mathbf{p}) * h_R(t) \tag{3}$$

where h_T, h_{Rm} and h_R are the transmitter, room and receiver response respectively. This model is visualised in Fig. 3. For fixed parameter vector $\mathbf{p}$, the model is linear.

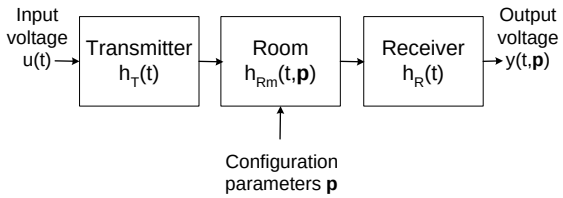

Fig. 3. System model of Eq. 3 shown as a series connection of transmitter, room, and receiver impulse responses.

4 Method

In this section the *signature matching* method will be presented. It can estimate the position of a mobile device in a room, based on a measurement using a single base station. Section 4.1 discusses what information the line-of-sight peak of the measured signal can provide. The algorithm is given in section 4.2. Section 4.3 shows how signatures can be matched, and finally section 4.4 discusses computational complexity and robustness of the method.

4.1 Line-of-sight measurement

Measurement of the line-of-sight (LoS) distance between base station and mobile device gives valuable information about the position of the mobile device. To obtain such a measurement, we assume that transmitter and receiver have

mutual time synchronisation by an RF link as e.g. in the Cricket [1] system. Figure 4 shows a front view of an empty room. For now, we assume that the fixed transmitter Tx near the ceiling acts as a base station and the mobile device Rx as a receiver. The LoS distance is visualised as a line between them. The partial sphere surface S shows the possible positions of Rx, if nothing but the LoS distance and the coordinates of Tx in the room are known. The LoS distance can

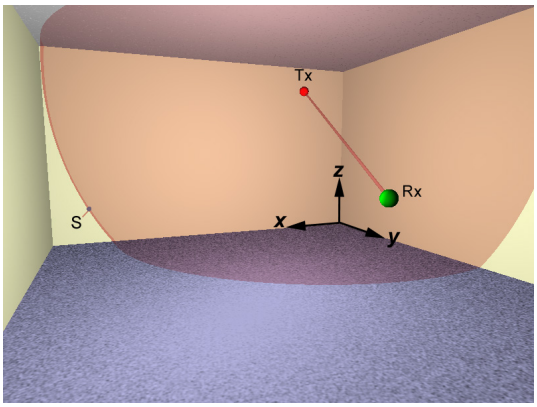

Fig. 4. 3D view of a room with transmitter Tx and receiver Rx.

be obtained by a straightforward first-peak detection on the measured signature, as demonstrated later in section 5.3.

However, a measurement of the LoS distance may fail due to blocking of the path between transmitter and receiver. Then, a reflection (arriving later) may be mistakenly seen as the LoS. This causes errors in position estimates, just like in current state-of-the-art ultrasonic positioning systems. Within the scope of this paper, a clear LoS path is assured by measuring in an empty room. In non-empty rooms, a higher probability of line-of-sight can be expected when placing the transmitter near the ceiling, because most obstacles are nearer to the floor.

4.2 Signature matching algorithm

The signature matching algorithm takes a measured signature vector $\mathbf{s}$ as input and outputs a position estimate $\hat{\mathbf{x}}$ of the mobile device. However, certain parameters must be known before the algorithm can be executed. The first group of parameters are the configuration parameters, describing the physical circumstances within the room. They were represented as parameter vector $\mathbf{p}$ in section 3.3. The room size (part of $\mathbf{p}$) can be obtained by manual input or estimated through echo measurements by the base station. If reflection factors Γ are not exactly known they have to be estimated. Furthermore the 3D position and orientation of the base station should be known. Finally we need the orientation vector $\mathbf{v}_R$ of the transducer mounted on a mobile device to be approximately

known. $\mathbf{v}_R$ is a 3D vector that should be seen as the 'pointing direction' of the transducer. There are three options to obtain $\mathbf{v}_R$, as will be discussed in section 4.4. The second group of parameters are the algorithm parameters. These include the grid spacing Δx (see step 2 in the algorithm) and the choice of time interval $[t_0, t_1]$ of the measured signal that we intend to use for matching.

For each measured signature $\mathbf{s}$ the following algorithm is executed:

1. From the measured signature $\mathbf{s}$ detect the line-of-sight peak at a distance d_{LoS} as explained in section 4.1.
2. Construct a partial sphere surface S (as shown in Fig. 4) bounded by the room volume, having radius d_{LoS}. Construct N_p regularly spaced 3D *candidate positions* $\mathbf{x}_i$ with $i = 1 \ldots N_p$ on surface S according to a pre-defined grid. The *grid spacing* parameter Δx represents the euclidean distance between adjacent candidate positions. Δx can be varied, depending on accuracy needs.
3. Start with candidate position $i := 1$. Set vector $\mathbf{m}$ empty.
4. For candidate position $\mathbf{x}_i$ and mobile device orientation vector $\mathbf{v}_R$, calculate the *expected signature* $\mathbf{s}^e$, using the system model (section 3.4) and signature processing (section 5.1).
5. Compare expected signature $\mathbf{s}^e$ to the measured signature $\mathbf{s}$ and compute a *match value* m expressing the amount of matching. Store m into vector element $\mathbf{m}(i)$. Possible matching methods are listed in section 4.3.
6. Proceed to the next candidate position $i := i + 1$, and repeat steps 4-6 while $i \leq N_p$.
7. Find index j with the highest match value in $\mathbf{m}$, $j = \max_i \mathbf{m}(i)$. The estimated position of the mobile device is the candidate position j at position coordinate $\mathbf{x}_j$.

The outcome is a position $\mathbf{x}_j$ whose simulated signature looks most like the measurement. Therefore, $\mathbf{x}_j$ is chosen in step 7 as a likely 3D position of the mobile device.

4.3 Comparison metrics

We define a *comparison metric* as an expression, involving two signature vectors $\mathbf{x}$ and $\mathbf{y}$ to compare, with a real value outcome m. A good comparison metric has the property that the maximum value of m, for all signatures $\mathbf{x}$ and $\mathbf{y}$ to compare, is associated with a 'best match' of the two signatures. In other words, the higher the outcome, the more $\mathbf{x}$ looks like $\mathbf{y}$. Step 5 of the signature matching algorithm requires such a match value.

Many comparison metrics are possible, for example mean-squared error, probabilistic comparison approaches, or pattern matching. The first metrics we tried were based simply on mean absolute difference between the signatures, because it can be calculated quickly. These metrics can be described by an expression M_q:

$$M_q(x, y) = -\frac{1}{N} \sum_{k=1}^{N} |x(k) - y(k)|^q \tag{4}$$

where q is a parameter to be chosen. The best match occurs when $\mathbf{x} = \mathbf{y}$, yielding maximum match value $M_q = 0$. M_1 is the mean absolute error metric and M_2 the mean squared error metric. Other comparison metrics are currently in development. For example, one such metric is based on the cross-spectrum between two signatures.

4.4 Discussion

The method and algorithm as presented, should be viewed as an initial result. Therefore, a computational complexity analysis was not made yet. Some remarks about the performance of our implementation will follow in section 5.1.

The configuration parameters for the algorithm are contained in parameter vector $\mathbf{p}$ (see section 3.3). Since parameters are measured or estimated, they will likely contain errors. Ideally the sensitivity of the algorithm to such errors should be low. An analysis of sensitivity has not been performed yet. Also for the algorithm parameters (listed in section 4.2) an analysis still needs to be done to determine optimal parameter values.

A drawback of the method is that the mobile device orientation $\mathbf{v}_R$ has to be known. At first sight nothing seems known about this orientation. However, we suggest three methods to obtain it. First, the orientation could be 'fixed by design'. An example is a remote control unit that is mostly lying horizontally on a table surface with the transducer pointing up. A second option would be to estimate an orientation, making use of characteristics of the measured signature. Methods to do so are in development. A third option is to use gravitational and/or inertial orientation sensors within a mobile device.

5 Experimental

The signature matching method has been implemented as a measurement setup, with all processing in software. The current implementation was built for two underlying goals. The first was to validate the room model as described in section 3.3 against a real empty room. The second goal was to realistically emulate an ultrasonic single-base-station positioning system, that makes use of the signature matching method. Then its performance could be tested in several room conditions. Section 5.1 describes the implementation, section 5.2 lists the experimental procedure and section 5.3 gives results.

5.1 Implementation

A choice that had to be made is whether the base station is a transmitter or a receiver. It was chosen to be a transmitter, which allows unlimited mobile receivers without risk of acoustic interference. The base station was implemented as a transmitter attached to a pole. The pole can be placed within a test room at positions close to walls or the ceiling. One mobile device was implemented

as a receiver attached to a pole. It can be moved around to measure at various positions and orientations in 3D space.

The remainder of this section will describe the measurement setup, the signal processing operations that produce a *signature*, and finally the implementation of the signature matching algorithm.

Measurement setup. The measurement setup is shown in Fig. 5. One transmitter and one receiver are connected to a measurement PC. Burst-like waveforms for output $u(k)$ are generated by MATLAB® [13] and sent to an output DAC. The analog output drives the 40 kHz Quantelec SQ-40T transmitter within ± 3 V at 500 kHz sampling rate. The acoustic signal propagates inside the room, and is recorded by a Quantelec SQ-40R receiver. The weak electrical signal is amplified, and filtered by a 30-100 kHz bandpass filter to remove electrical noise. The ADC samples at 12-bit resolution at 250 kHz and sends the data $y(k)$ to MATLAB. All units are connected by coaxial cables. No special shielding was used for the transducers.

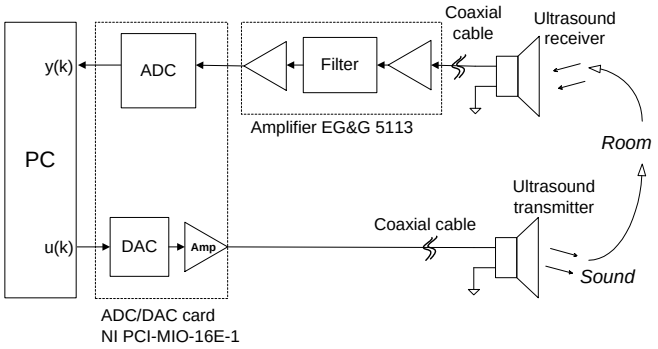

Fig. 5. Measurement setup.

Signal processing. The measured signal $y(k)$ can not be used directly as input to the positioning algorithm. A number of operations are performed to generate *signature data*, which forms the input to a positioning algorithm. The signature contains all relevant information of the measurement in a more convenient and compact form. Figure 6 shows the operations performed on the (discrete) measured data samples $y(k)$. The first step is a cross-correlation filter, that performs a matched filtering operation to remove noise. The template $t(k)$ is the signal as expected to arrive from a single acoustic ray, obtained using the transducer model in section 3.1. The second step demodulates the amplitude envelope from its $f_c = 40$ kHz carrier frequency. Since the bandwidth of the demodulated signal is very low, it can be safely low-pass filtered and downsampled by a factor

5 to a new sampling frequency $f_s = 50$ kHz. The fourth step is attenuation compensation, which compensates the typical drop in signal amplitude of ultrasound over distance. It can be calculated as explained in section 3.2. Without this step, a signature's appearance would be dominated by the first few early-arriving reflections, which are higher in amplitude than late-arriving ones. The compensation step allows for a fair comparison between two signatures when using amplitude-based metrics as in Eq. 4.

The result is a signature $s(k)$ which shows a typical peak and valley pattern, where each peak signifies the arrival of one or more acoustic xrays at the receiver at that moment in time. The discrete-time signature $s(k)$ can be written also as a signature vector $\mathbf{s}$. For an example signature see Fig. 2.

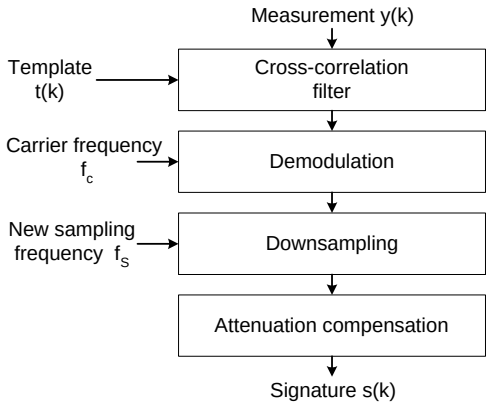

Fig. 6. Signal processing operations to obtain a signature.

Algorithm implementation. The signature matching algorithm was implemented in MATLAB, using the M_1 metric for signature comparison. The most complex part of the algorithm is the simulation of signatures $\mathbf{s}^e$ for each of the candidate positions. Implementation details are not shown, but the major computational bottleneck will be discussed now.

The highest load is imposed by the simulation of the N_p signatures according to Eq. 3. Fourier transforms were used to calculate it in the frequency domain, for increased speed. Two N-point FFT operations and one N-point vector multiplication are then needed per signature, where N=2180 for the current implementation. Typical values for N_p that were tried range from 500 to 20000. To improve performance N_p can be set lower, by choosing a coarser candidate grid size (i.e. $\Delta\mathbf{x}$ higher, see section 4.2) or by excluding certain positions from the candidate set (e.g. positions near the ceiling that are never reached). An interesting improvement would be an iterative approach, that first selects the

promising areas in 3D space having high match values, and only executes the algorithm for a limited set of candidate positions located in the promising areas.

5.2 Experimental procedure

All experiments were performed in an empty office room. An empty room was chosen to verify the acoustic empty room model. Also, an empty room represents the best-case condition for any positioning system. Experiments in a room with obstacles, a more difficult and realistic room condition, are not described in this paper.

The room size is 3.73 m by 7.70 m and 2.97 m high. Some irregularities are present in the form of windows, window-ledges, a door, radiator, a tap and sink, and ceiling-embedded lighting units. A 3D cartesian coordinate system was defined as shown in Fig. 4. The base station position $(0.95, 0.04, 2.95)$ near the ceiling was used, to mimic typical ceiling placement for non-empty rooms, as mentioned in section 4.1. The receiver was placed at several positions in the room which will be shown later in section 5.3. The height of the receiver was set around 1.3 meter, to mimic a typical height for a mobile device that is carried around in a user's hand. The orientation of the receiver was always set parallel to the negative y axis, i.e. $\mathbf{v}_R = (0, -1, 0)$. Measurements were taken at each position. During measurements, no large obstacles or people were present in the room and the door was kept closed.

5.3 Results

The results of initial experiments are presented in this section. First, a single measurement for a receiver position will be examined in detail. A graph will be shown that visualises the output vector $\mathbf{m}$ of signature match values, as generated by the algorithm. Then, for the rest of the measurements only the end results of 3D position estimation will be shown.

One measurement will be examined in detail now. The measured signature $\mathbf{s}$ is shown in Fig. 2. First, the line-of-sight distance is measured (step 1 of the algorithm). A standard peak-detection algorithm estimates the first peak at a distance $d_1 = 2.89$ m, similar to the true distance 2.88 m. A sphere surface S is constructed (step 2) with radius d_1 and centre x_T. Each position on S can now be described in a spherical coordinate system (with origin x_T) by a coordinate (θ, ϕ, r) with $r = d_1$. This way we translate the position estimation problem from 3D cartesian coordinates to a 2D vector (θ, ϕ) to be estimated. A grid spacing $\Delta\theta = 0.017$ is chosen for both θ and ϕ, which corresponds to a variable grid spacing Δx in cartesian coordinates. For this grid spacing it holds that $\Delta x \leq 2 \cdot d_1 \cdot \sin(0.5\ \Delta\theta) = 0.05$ meter. So the candidate positions are at every 5 cm (or closer) within the room. In total $N_p = 11067$ candidate positions exist on the sphere surface within the room.

Starting at candidate position 1, the expected signature is calculated (step 4), a match to the measurement is performed and stored (step 5), and this is repeated for all candidate positions (step 6). The result is a collection of

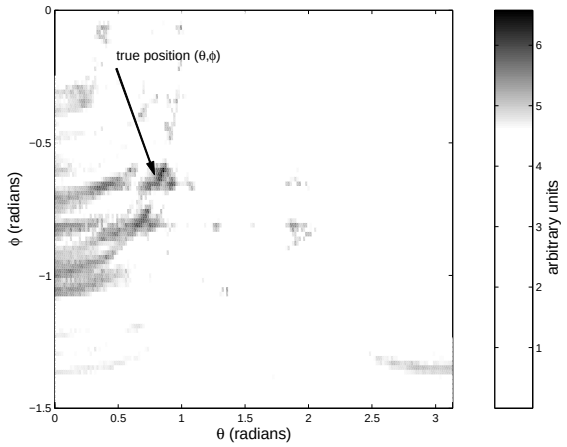

Fig. 7. Visualisation of the result of algorithm steps 1-6. Signature match values are represented by shaded pixels. Darker shades have higher match values. The arrow marks true receiver position.

match-values which are a function of the two coordinate parameters θ, ϕ. It is insightful to represent match value as a shade of grey and plot it in a 2D graph with axes (θ, ϕ). This is shown in Fig. 7, where the higher match values are shown as darker shades of grey. The arrow marks the true mobile receiver position. The area surrounding the true position is darkest grey, which means the signatures there match the measurement best. The maximum match value can now be picked from these results (step 7). Best match is candidate position $(\theta, \phi, r) = (0.849, -0.611, 2.89)$, corresponding to cartesian coordinate $\hat{\mathbf{x}} = (2.51, 1.81, 1.30)$. The 3D distance error $|\hat{\mathbf{x}} - \mathbf{x}_R|$ with respect to the true position $\mathbf{x}_R = (2.60, 1.70, 1.27)$ is just 15 cm.

The algorithm was executed for 20 measurements in total at various positions in the test room. These positions are shown as circles in Fig. 8, which contains an X/Y top view of the room. In the same graph, the estimated positions are shown by lines pointing from the encircled true positions towards the estimated positions. In Fig. 9 the same measurements are shown as a bar graph where the vertical axis represents the 3D estimation error $|\hat{\mathbf{x}} - \mathbf{x}_R|$. It can be seen that accuracy is usually better than 20 centimeters, except for positions 2 and 11 which have a relatively large position error. The reason for these errors is the topic of further research.

6 Conclusions

Based on the experimental work it can be concluded that measured ultrasonic signals contain much more information than just the transmitter-receiver line-of-sight distance. This information is contained in a measured pattern, the *sig-*

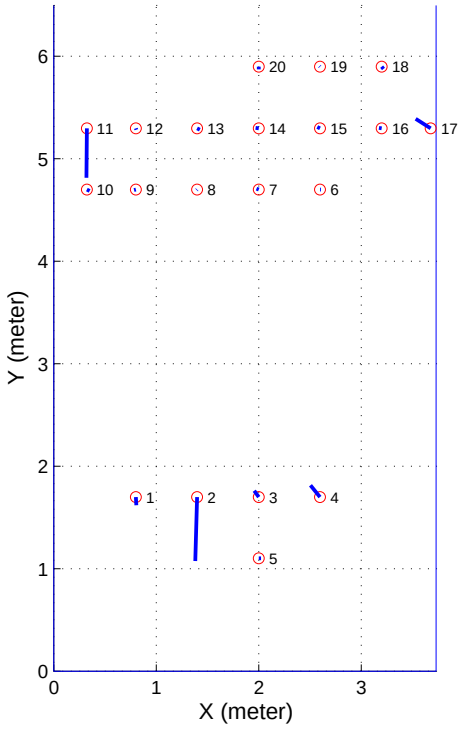

Fig. 8. Top view of the test room, showing 20 measurement locations (encircled). The position estimates per position are shown by the tips of the solid lines.

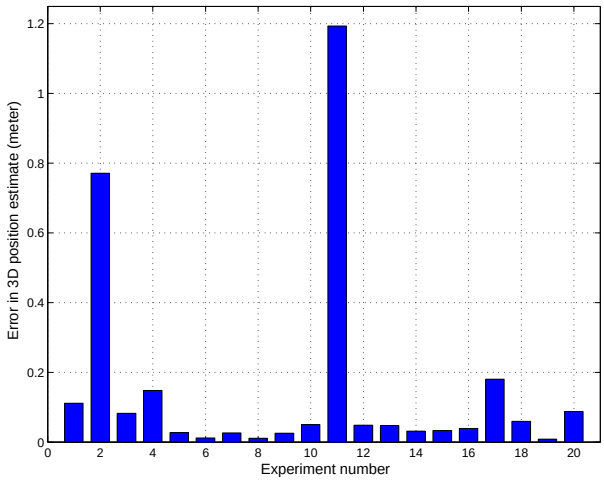

Fig. 9. 3D positioning results over 20 experiments. The vertical axis plots 3D position estimation error.

nature. The signature consists of amplitude peaks, that are caused by acoustic reflections. It was shown that the signature can be predicted by an acoustic room model. We propose to use the information contained in the signature to perform 3D device position estimation, using just a single base station per room. A method called *signature matching* was designed and implemented for this purpose. It was shown by initial experiments that the acoustic model is accurate enough to use for 3D position estimation, for the case of an empty room.

The method described in this paper is not yet mature. In future work a number of steps will be taken: Firstly, the method will be tested more thoroughly, specifically in realistic non-empty room conditions. Secondly the computational complexity of the method needs to be improved. Thirdly, a sensitivity analysis has to be performed to find out the effect of errors in the method's input parameters. Fourthly, an extension of the method, based on transducer arrays, is under development. Such an array allows a base station to get more information about the direction of mobile devices, thus enabling more robust position estimates.

Acknowledgments

The authors would like to thank S. Egner for signal processing support, and the other members of the PHENOM project team: Y. Burgers, E. van den Hoven, N. de Jong, Y. Qian, D. Teixeira and E. Tuulari.

References

1. Priyantha, N., Miu, A., Balakrishnan, H., Teller, S.: The Cricket Compass for Context-Aware Mobile Applications. In: Proc. ACM Conf. on Mobile Computing and Networking (MOBICOM). (2001) 1–14
2. PHENOM project: www.project-phenom.info (2003)
3. Ni, L., Liu, Y., Lau, Y., Patil, A.: LANDMARC: Indoor Location Sensing Using Active RFID. In: Proc. IEEE Int. Conf. on Pervasive Computing and Communications (PerCom). (2003)
4. Prasithsangaree, P., Krishnamurthy, P., Chrysanthis, P.: On Indoor Position Location with Wireless LANs. In: Proc. IEEE Int. Symp. on Personal, Indoor and Mobile Radio Communications (PIMRC). (2002) 720–724
5. Addlesee, M., Curwen, R., Hodges, S., Newman, J., Steggles, P., Ward, A., Hopper, A.: Implementing a Sentient Computing System. IEEE Computer **34** (2001) 50–56
6. Hazas, M., Ward, A.: A Novel Broadband Ultrasonic Location System. In: Proc. Int. Conf. on Ubiquitous Computing. (2002) 264–280
7. InterSense: IS series high precision trackers, www.isense.com (2003)
8. Ziomek, L.: Fundamentals of Acoustic Field Theory and Space-Time Signal Processing. CRC press (1995)
9. Crocker, M.: Handbook of Acoustics. J. Wiley & Sons (1998)
10. Kuttruff, H.: Room Acoustics. 3rd edn. Elsevier (1991)
11. ISO: Standard 9613-1; Acoustics - Attenuation of sound during propagation outdoors (part 1), www.iso.ch (1993)
12. Allen, J., Berkley, D.: Image Method for Efficiently Simulating Small-Room Acoustics. J. Acoust. Soc. Am. **65** (1979) 943–951
13. Mathworks: MATLAB version 6 (R13), www.mathworks.com (2003)